Corrosion Science xxx (xxxx) xxx–xxx

Contents lists available at ScienceDirect

Corrosion Science

journal homepage: www.elsevier.com/locate/corsci

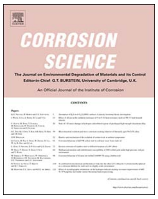

Investigation on early formation and evolution of oxide scales on ferritic–martensitic steels in supercritical water

Yanhui Li[a,b], Shuzhong Wang[a,*], Panpan Sun[a], Jiaoqiao Yang[a], Xingying Tang[c], Donghai Xu[a], Yang Guo[a], Jie Yang[b], Digby D. Macdonald[b]

[a] *Key Laboratory of Thermo-Fluid Science and Engineering of MOE, School of Energy and Power Engineering, Xi'an Jiaotong University, Xi'an, Shaanxi 710049, China*
[b] *Department of Nuclear Engineering, University of California at Berkeley, Berkeley, CA 94720, USA*
[c] *School of Marine Sciences, Guangxi University, Nanning, Guangxi 530004, China*

ARTICLE INFO

Keywords:
A. Steel
B. AFM
B. SEM
B. XPS
C. High temperature corrosion
C. Oxidation

ABSTRACT

Early oxidation characteristics of ferritic-martensitic steel T91 in supercritical water (SCW) from 1 h to 120 h were investigated. Relative to austenitic steels, occurrence of each oxidation stage for T91 was delayed. Both inner Cr-rich layer and outer magnetite layer formed even after a 1h-exposure at 540 °C, implying their almost simultaneous formations. Several assembled-pore lines were observed in the inner layer. Abundant pores accumulated at the boundary between the inner/outer oxide layers in steam, while mainly along the inner/diffusion layer interface in SCW, due to lower difference between iron diffusion through the inner and outer layers for the later.

1. Introduction

Ferritic-Martensitic (F-M) steels with chromium contents between 9 and 12 wt.% and with low nickel content, have been extensively employed as structural materials in the high-temperature regions in fossil-fired thermal and nuclear power plants [1,2]. Because these steels generally exhibit good high temperature strength and creep resistance, high thermal conductivity, low swelling and activation under irradiation, low susceptibility to stress corrosion cracking and modest corrosion resistance. The corrosion behavior of F–M steels in supercritical water (SCW) has been widely investigated in recent years [1,3–11]. Reported literature indicates that typical oxide scales formed on the F-M steels after a long-term exposure in SCW, generally comprises an outer oxide layer with a larger number of columnar Fe_3O_4 grains, an inner oxide layer with a mixture of small-sized, equiaxed Fe_3O_4 and $FeCr_2O_4$ particles, and possibly an additional feature of a diffusion layer [1,2,4,10,12,13]. Yi [3], Yin [14], Bischoff [6] pointed out that the oxidation mechanism of F-M steels in SCW is similar to that in gaseous environment where only solid growth takes place and the dissolution of the oxide scales into SCW is negligible, because of the low dielectric constant. The inner/outer layer interface is located at the original metal surface [5,6,8], which implies a particular relationship between the transport numbers for cations and oxygen vacancies in barrier layer. Thus, the outward migration of iron gives rise to the formation of the outer layer and an inward migration of oxygen carriers forms the inner, barrier layer [6]. The rate-limiting step during the steady-state growth stage of the oxide scales is the outward migration of iron interstitials through the barrier layer rather than the inward transport of oxygen-carriers [6,8,9].

Most of the previous experiments were typically carried out with exposure times above 100 h, focused primarily on cross-sectional structure of the oxide scales on F-M steels in SCW, and sough to define the thickening mechanism of the scales. However, these experiments were incapable of exploring the early oxidation behavior of the steels, because the films generally formed at over times of less than 100 h. Studies over < 100 h are very important because they may provide valuable guidance to further understand the formation process of scales and to improve the oxidation resistance of the steels. Our previous paper explored the early formation mechanism of oxide scales grown on austenitic stainless steel TP347H in SCW at 540 °C and 25 MPa for 7–120 h [15]. The results indicated the formation priority of the continuous inner Cr-rich spinel layer relative to the outer magnetite subscale. At present, few studies have explored the earlier oxidation of F-M steels in SCW. Tan et al. [9] reported that for the HCM12A samples exposed to SCW at 500 °C for 1 h, the thicknesses of the inner- and outer- layers were already 0.8 μm and 1.0 μm, respectively. In addition, little information was available concerning the difference between the oxide scales formed in SCW and high-temperature steam, and little information was forthcoming on formation-evolution of pores within/on the oxide scales. The studies performed by Ren et al. [16] indicated

---

[*] Corresponding author.
E-mail address: szwang@xjtu.edu.cn (S. Wang).

https://doi.org/10.1016/j.corsci.2018.02.036
Received 13 October 2017; Received in revised form 25 January 2018; Accepted 17 February 2018

Please cite this article as: Li, Y., Corrosion Science (2018), https://doi.org/10.1016/j.corsci.2018.02.036

that the pore density on the oxide surface increased with an increase in exposure time, while Zhang et al. [4] concluded exactly the opposite. Yang et al. [17] found that surface pores initiated at short exposure times but diminished with an increase in exposure time.

Among the fully commercialized, 9 wt.% Cr steels, the T91 steel has the highest yield stress (yield stress/safety factor) and has been used world-wide for header and steam piping in ultra-supercritical fossil plants operating up to 593 °C. This steel has been identified as one candidate material for fuel cladding and core structural components in the Generation IV supercritical water-cooled nuclear reactor concept [2,3]. This paper aims to explore the earlier oxidation mechanism of the typical F-M steel T91 exposed to SCW from the initial oxide nucleation to the formation of the complete, protective oxide scale. Based upon the obtained oxidation kinetics data forT91 in SCW at 540 °C and 25 MPa and in steam at 540 °C and 9.9 MPa (traditional operating parameters for fossil power plant), this paper initially focuses on characterizing the early evolution of the T91 surface morphology, the oxide phases formed, and changes in the chemical composition with increasing exposure times from 1 h to 120 h in SCW at 540 °C, using a series of analytical techniques suitable for ultrathin scales. Next, the effect of temperature on the oxidation characteristics of T91 steel after a 40 h-exposure in SCW, and the structure difference of oxide scales grown in SCW and steam for 120 h, are systematically investigated. The related early oxidation process of T91 steel in SCW, and the formation and evolution of pores within the oxide scales are also discussed.

2. Experimental

Commercial, hot-rolled tubes of Ferritic-martensitic steel T91 was used in this study. The steel's nominal chemical composition is listed in Table 1. Rectangular samples (8 mm × 5 mm) with a thickness of 3 mm were cut from the as-received materials, with the 8-mm long side parallel to the tube axis. The samples were mechanically ground with SiC abrasive paper up to 2000 grits, and then polished to a ~1 μm finish with diamond paste prior to exposure in SCW. Deionized water with a conductivity of < 0.1 μS/cm was used in the experiments, and it was continuously deaerated with nitrogen while monitored by a dissolved oxygen analyzer to maintain the dissolved oxygen at a level of approximately 40 ppb, which is the operating condition (30–150 ppb O_2) in supercritical power plants in China.

The oxidation behaviors of T91 samples were investigated in high-temperature steam at 9.9 MPa and 540 °C (traditional operating parameters for fossil power plants), and in 25 MPa SCW at four temperatures of 580 °C, 540 °C, 465 °C and 390 °C. There are two experimental devices used in this study: a SCW test system and a capsule-tubular furnace apparatus. Data points with the exposure time of 10 h and above were gained by the SCW test system. In order to avoid interference of the preheating process on the experiment, during which the effective exposure time was only 1 h, the quick-heating capsule-tubular furnace apparatus was also constructed. The SCW test system comprises a high-temperature autoclave, a PID temperature controller, a metering pump, and auxiliary instruments, such as a heater. The detailed construction and experimental procedures have been described in our previous articles [18,19]. For the capsule-tubular furnace apparatus, the capsule was made of Inconel 625, which has a length of 100 mm with inner and outer diameters of 6 mm and 10 mm, respectively. After directly placing the samples in one capsule, the capsule was filled with a predetermined amount of the experimental water and then sealed by using a 6 mm diameter screw. Then, the capsule was exposed in a tubular furnace at 540 °C for a residence time of 1 h. Preliminary experiments showed that the capsule can be heated to 540 °C and ~25 MPa within 5 min, so that it is acceptable to ignore the heating-up time. In all experiments, two or three samples were used for determining each data point in producing the weight gain curves; in each case, the weight gain was normalized by the surface area of the samples (weight gain per unit area).

Table 1
Nominal chemical composition of T91 steel (wt.%).

C	Cr	Fe	Mo	Mn	Ni	Nb	Others
0.097	8.91	Bal.	0.96	0.48	0.35	0.08	0.65Si,0.05N

An electronic balance (Satorius) with a sensitivity of 0.01 mg was used for gravimetry before and after an experiment. The microstructure and composition of the exposed samples were characterized by a variety of analytic methods, such as scanning electron spectroscopy (SEM, JSM-6390) equipped with an energy dispersive X-ray spectroscopy (EDS), X-ray Diffractometer (XRD, Panalytical X'PertProMPD), Atomic Force Microscopy (AFM: NT-MT SOLVER NEXT*), Raman Microscopy (Horiba LabRAM HR 800), and X-Ray Photoelectron Spectrometry (XPS: Kratos AXIS-ULTRA DLD).

3. Results

3.1. Oxidation kinetics

Weight gains (Δ*w, in* mg cm^{-2}) of the T91 samples exposed to SCW and steam at 540 °C for 1 h, 10 h, 20 h, 40 h, and 120 h, and the fitted plots of Δ*w* versus exposure time (t, in hours), are shown in Fig. 1. The weight gains of the T91 samples in SCW were obviously higher than those of the specimens exposed to the high temperature steam, while the weight gains all increased with an increase in exposure time for the two environments [5]. Oxidation rates can be characterized by near-parabolic laws with similar oxidation rate constants, implying that the oxidation process of steel T91 in two environments may be controlled by a similar predominant diffusion process [6,20]. However, in steam the time exponent was 0.35, which is smaller than that obtained in SCW (about 0.42), suggesting that relatively fewer defects exist within protective layer of oxide scales for the former [5], assuming that the diffusion of defects is rate-controlling. In order to comparatively analyze the temperature effects on early weight gains of F-M steels, some Δ*w* data and kinetic curves of typical F-M steels at several temperatures obtained from available literatures [4–6,9], are also shown in Fig. 1. In this paper, the experimental results are consistent with the extrapolated curves. In SCW, the weight gains of common F-M steels at 540–550 °C is around two times higher than that obtained at 500 °C, while the 600 °C data generally are about 5–6 times larger than those at 500 °C. The increasing rate of Δ*w* (*d*Δ*w/dt),* for T91 steel in SCW at 540 °C is also presented in Fig. 1. The increasing rate first decreases significantly in the initial stage, and then falls slowly with exposure time, eventually the curve of increasing rate tends to a constant. Depending on the magnitude of second derivative of Δ*w* in exposure time ($d^2\Delta w/dt^2$), the early oxidation of F-M steels in SCW at 540 °C can be categorized into

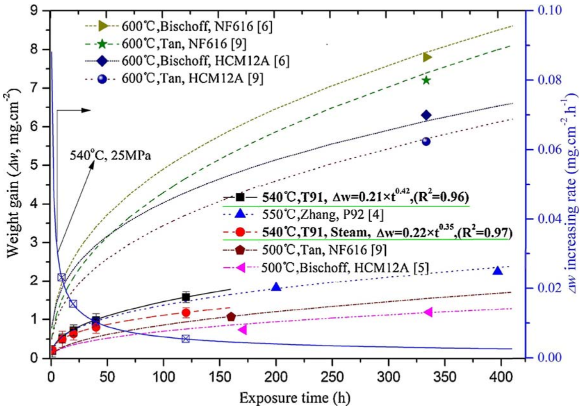

Fig. 1. Weight gain (Δ*w*) as a function of exposure time (t) for F-M steels exposed to steam (9.9 MPa and 540 °C) and SCW (25 MPa and 500 °C, 540 °C, 550 °C, and 600 °C).